Communication

Crystalline Superlattices from Single-Sized Quantum Dots

Nanfeng Zheng, Xianhui Bu, Haiwei Lu, Qichun Zhang, and Pingyun Feng

J. Am. Chem. Soc., **2005**, 127 (34), 11963-11965• DOI: 10.1021/ja053588o • Publication Date (Web): 09 August 2005

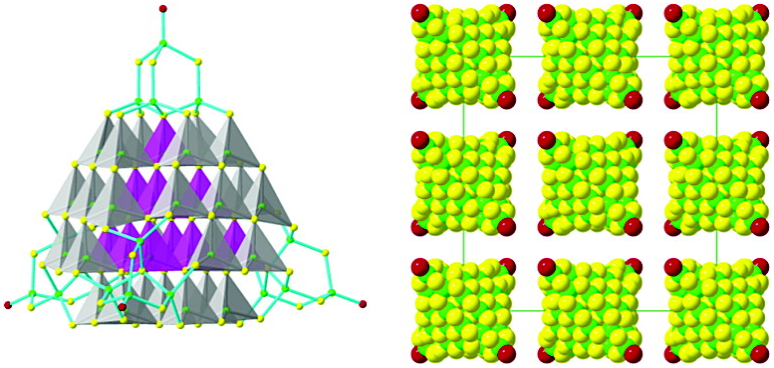

J|A|C|S
COMMUNICATIONS

Published on Web 08/09/2005

Crystalline Superlattices from Single-Sized Quantum Dots

Nanfeng Zheng,† Xianhui Bu,‡ Haiwei Lu,† Qichun Zhang,† and Pingyun Feng*,†

Department of Chemistry, University of California, Riverside, California, 92521, and Department of Chemistry and Biochemistry, California State University, 1250 Bellflower Boulevard, Long Beach, California, 90840

Received June 1, 2005; E-mail: pingyun.feng@ucr.edu

With uniform cluster size and long-range periodic ordering, chalcogenide clusters and their superlattices allow the study of quantum confinement effects and collective properties at the lower size limit of three-dimensionally confined quantum dot structures.[1−5] Chalcogenide clusters can also serve as artificial atoms for the construction of molecular architectures that integrate uniform porosity and semiconductivity and may have applications as size- or shape-selective photocatalysts, sensors, etc.[6−11] The study of chalcogenide quantum structures may also help to understand the formation mechanism and structures of biogenic metal chalcogenide nanocrystallites produced by various organisms to sequester toxic transition metals, such as Cd, Pb, and Hg, and excess nontoxic transition metals.[12]

To effectively utilize size-dependent properties of quantum dots, the control of the size dispersity is essential in the synthesis of semiconductor nanocrystals. An ideal situation would be the synthesis of quantum dots with a precisely controlled number of atoms and shape. Unfortunately, quantum dots developed so far generally contain structural irregularity at the atomic level and could not usually be made with a precise number of atoms. Prior to this work, small II−VI chalcogenide clusters have been synthesized with the largest cluster (∼15 Å) containing 32 Cd^{2+} sites and 50 chalcogen sites.[13−17] Larger clusters have been reported as peptide-capped intracellular particles of 20 Å diameter, but detailed structures of such biogenic clusters remain unclear.[12]

Here, we report a general one-step solvothermal approach that allows the synthesis and crystallization of large single-sized tetrahedral quantum dots.[18] For the first time, tetrahedral II−VI chalcogenide clusters with over 100 metal−chalcogen sites have been prepared. The crystal structures of the clusters with 138 atom sites and fewer have been determined by single-crystal analysis. Clusters larger than 138 metal−chalcogen sites have also been made and were characterized by X-ray powder diffraction (XRD) and optical absorption. The variation in the cluster size, composition, and topology leads to a rich family of single-sized quantum dot structures, which upon self-assembly form highly ordered three-dimensional crystalline superlattices.

New materials reported here are denoted as MOL-*p*, where *p* is an integer indicating a particular structure type that is independent of chemical compositions (Table 1). For simplicity in discussion and to emphasize the size of the cluster, we also use general terms, such as Cd-17, Cd-32, and Cd-54, to refer to a nanocluster that contains the specified number of metal cations.

Crystals of these nanoclusters can be reversibly dissolved and recrystallized from solvents, such as dimethylformamide (DMF). Drop-casting or spin-coating their solutions on different substrates led to the formation of thin films that showed the same XRD pattern as corresponding polycrystalline samples, suggesting that tetrahedral clusters remain intact upon dissolution.

Topologically, clusters reported here are related to a series of clusters termed capped tetrahedral clusters, denoted as C*n*.[19] Each C*n* cluster consists of a core that is a regular fragment of the cubic zinc blende-type phase and four corner barrelanoid cages possessing the characteristics of the hexagonal wurtzite-type phase. The first member (denoted C1) in this series contains 17 metal sites (e.g., $[Cd_{17}S_4(SPh)_{28}]^{2-}$), while the second member (C2) contains 32 metal sites (e.g., $Cd_{32}S_{14}(SPh)_{36}\cdot 4DMF$). One distinct structural feature of C*n* clusters is that there is an open cleft along each edge of the cluster. Even though C2 clusters were first made more than one decade ago, larger homologues remained elusive until this work. Here, the largest cluster (20 Å in size) determined from single-crystal analysis contains 54 Cd^{2+} sites and 84 anionic sites. XRD and optical studies indicate that even larger clusters have been synthesized.

One unique advantage demonstrated here is the possibility to probe the structural details of nanocrystals at the atomic level by single-crystal diffraction. This ability has allowed us to discover an interesting structural isomerism that has not been recognized in colloidal nanocrystals or biogenic Cd−S nanocrystallites. For C*n* clusters, each barrelanoid cage (Cd_4S_4) at one of four corners can be independently rotated by 60°, which results in four new series of tetrahedral clusters, denoted as C*n*,*m* clusters (for $n = 1$, only one corner can be rotated). The integer *m* refers to the number of corners that have been rotated in relation to those in parent C*n* clusters.

The $[Cd_{54}S_{32}(SPh)_{48}(H_2O)_4]^{4-}$ cluster reported here is, so far, the largest II−VI quantum dot determined by single-crystal diffraction (Figure 1A). The size of this cluster as measured between corner metal sites is about 20 Å, comparable to biogenic cadmium sulfide nanocrystallites reported earlier.[12] This cluster can be described as a hybrid between cubic zinc blende-type core and hexagonal wurtzite-type corners. At the center of the cluster is a regular supertetrahedral $[Cd_{10}S_{20}]^{20-}$ cluster. Using the nomenclature introduced earlier, the $[Cd_{54}S_{32}(SPh)_{48}(H_2O)_4]^{4-}$ cluster is denoted as C3,4.

Compared to C*n* clusters with open clefts, all four corners of the $[Cd_{54}S_{32}(SPh)_{48}(H_2O)_4]^{4-}$ cluster are rotated by 60°. Thus, open clefts in this new cluster are interrupted near corners. The corner rotation also converts six-membered rings (Cd_3S_3) between the second and third layers of the cluster (the corner metal site is considered as the first layer) from the chair form (the fundamental feature of the cubic zinc blende phase) into the boat form (one characteristic feature of the hexagonal wurtzite phase). Thus, the interface between the cubic core and the hexagonal corner is shifted by one atomic layer toward the center of the cluster in C*n*,*m* clusters.

The isomerization observed in the C3,4 cluster appears to be a rather common phenomenon, even though it has not been recognized in colloidal and biogenic nanocrystallites. We have also synthesized another type of cluster in which two corners in Cd-32 clusters are rotated. As shown in Figure 1B and Table 1, the Cd-

† University of California.
‡ California State University.

Table 1. A Summary of Crystallographic Data for Selected New Structures Synthesized in This Study[a]

name[b]	cluster	cluster composition	space group	*a* (Å)	*b* (Å)	*c* (Å)	*R*1
MOL-1 CdS−TMA	C3,4 CdS	$Cd_{54}S_{32}(SPh)_{48}(H_2O)_4^{4-}$	$F\bar{4}3c$	48.3440(7)	48.3440(7)	48.3440(7)	7.39
MOL-1 CdSeS−TPhP	C3,4 CdSeS	$Cd_{54}Se_{32}(SPh)_{48}(H_2O)_4^{4-}$	$P23$	24.0656(7)	24.0656(7)	24.0656(7)	8.65
MOL-1 CdS−TPhP	C3,4 CdS	$Cd_{54}S_{32}(SPh)_{48}(H_2O)_4^{4-}$	$F\bar{4}3c$	48.2476(31)	48.2476(31)	48.2476(31)	10.34
MOL-1 CdS−OTMA	C3,4 CdS	$Cd_{54}S_{32}(SPh)_{48}(H_2O)_4^{4-}$	$F\bar{4}3c$	48.36(3)	48.36(3)	48.36(3)	
MOL-1 CdCoS−TPhP	C3,4 CdCoS	$Cd_{54-x}Co_xS_{32}(SPh)_{48}(H_2O)_4^{4-}$	$F\bar{4}3c$	48.31(7)	48.31(7)	48.31(7)	
MOL-1 CdFeS−TPhP	C3,4 CdFeS	$Cd_{54-x}Fe_xS_{32}(SPh)_{48}(H_2O)_4^{4-}$	$F\bar{4}3c$	48.25(5)	48.25(5)	48.25(5)	
MOL-2 CdS−TPhP	C2,2 CdS	$Cd_{32}S_{14}(SPh)_{40}^{4-}$	$P2_1/c$	37.4751(76)	26.4821(55)	34.5044(68)	10.35
MOL-3 CdS	C1 CdS	$Cd_{17}S_4(SPh)_{26}(H_2NCSNH_2)_2$	$P3_221$	19.172(3)	19.172(3)	45.758(9)	9.31
MOL-4 CdSSe	C1 CdSSe	$Cd_{17}S_4(SePh)_{26}(H_2NCSNH_2)_2$	$R3c$	26.8878(38)	26.8878(38)	87.5531(175)	8.13

[a] Diffraction data were collected on a Bruker Apex CCD diffractometer with a Mo Kα X-ray source at 90−150 K. The structures were solved by direct methods and refined using XShell 6.2. The final full-matrix refinements were against F^2. $R(F) = \sum||Fo| - |Fc||/\sum|Fo|$ with $Fo > 4.0\sigma(F)$. For MOL-2 CdS−TPhP, $\beta = 99.123(8)°$. [b] TMA = tetramethylammonium, $C_4H_{12}N^+$; TPhP = tetraphenylphosphonium, $C_{24}H_{20}P^+$; OTMA = *n*-octyltrimethylammonium, $C_{11}H_{26}N^+$.

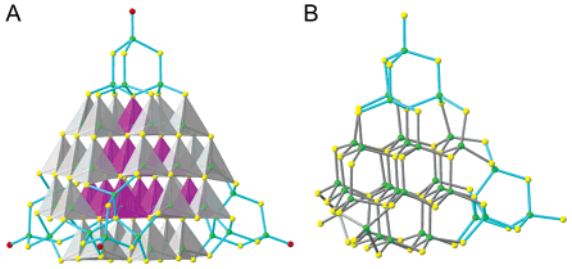

Figure 1. The structural diagrams of the tetrahedral clusters. (A) The C3,4 cluster $[Cd_{54}X_{32}(SPh)_{48}(H_2O)_4]^{4-}$ (X = S or Se). The central $[Cd_{10}X_{20}]^{20-}$ T3 cluster is shown as the purple tetrahedra. Gray tetrahedra represent CdS_4 units at the surface. Green sphere: Cd^{2+}; yellow sphere: S^{2-}; red sphere: H_2O. (B) The C2,2 cluster $[Cd_{32}S_{14}(SPh)_{40}]^{4-}$ with two terminal barrelanoid cages rotated. The rotated barrelanoid cages are highlighted by cyan-colored bonds.

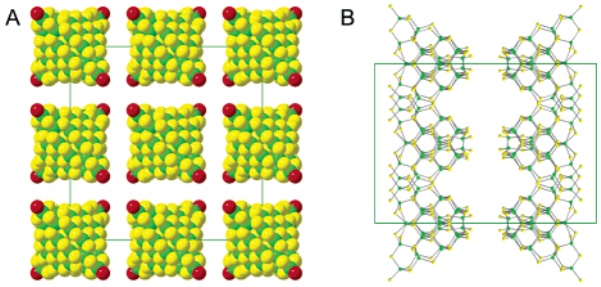

Figure 2. (A) In MOL-1 CdS−TPhP, C3,4 Cd-54 CdS clusters have a faced-centered cubic arrangement similar to the packing of Na^+ and Cl^- ions in the NaCl structure. (B) The packing diagram of C2,2 Cd-32 clusters in MOL-2 CdS−TPhP.

32 cluster in MOL-2 has two rotated corners and is denoted as the C2,2 cluster. Such isomerization phenomenon revealed by single-crystal analysis is of particular interest because it is generally not possible to detect them in colloidal or biogenic Cd−S crystallites.

By replacing thiourea with selenourea, we have also synthesized $[Cd_{54}Se_{32}(SPh)_{48}(H_2O)_4]^{4-}$, a core−shell-type C3,4 cluster. The reverse core−shell-type cluster (e.g., $Cd_{17}S_4(SePh)_{26}(H_2NCSNH_2)_2$ in MOL-4) can be made when thiophenolate ligands are replaced with selenophenolate ligands. It is also possible to incorporate magnetic transition metal cations (e.g., Co^{2+} and Fe^{2+}) into nanoclusters (Table 1), further increasing the diversity and potential applications of materials that may be realized through this synthetic approach.

Cd-54 clusters crystallize into the F-centered NaCl-type supercell structure with both Na^+ and Cl^- sites replaced by $[Cd_{54}S_{32}(SPh)_{48}(H_2O)_4]^{4-}$ clusters (Figure 2). Alternatively, Cd-54 clusters can also crystallize into primitive cubic structure (Table 1). In either case, the crystal is noncentrosymmetric (space groups: $F\bar{4}3c$ or $P23$).

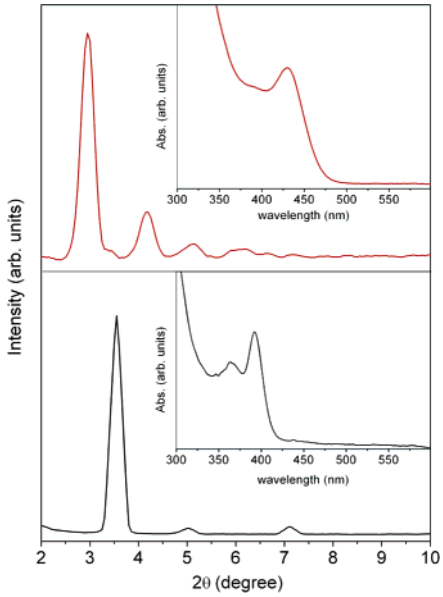

Figure 3. XRD and UV−vis spectra of MOL-1 CdSeS−TPhP and MOL-5 CdSeS−TPhP. (Top) XRD of MOL-5 CdSeS−TPhP. Its absorption spectrum in DMF is shown in the inset. (Bottom) XRD of MOL-1 CdSeS−TPhP; its absorption spectrum in DMF is shown in the inset.

The packing of large tetrahedrally shaped Cd-54 clusters leads to a large void space that is occupied by disordered charge-balancing species (e.g., $N(CH_3)_4^+$) and solvent molecules.

The synthetic approach for Cd-54 clusters is a general route for the synthesis and crystallization of tetrahedral clusters. Similar molecular crystals have also been grown from clusters of other sizes by using this approach (Table 1), demonstrating the broad applicability of our synthetic method in synthesizing crystals of quantum dots. The experimental evidences for clusters larger than Cd-54 were provided by X-ray powder diffraction and optical absorption studies. Single-crystal analysis, however, remains inconclusive, likely due to the orientational flexibility of clusters within the three-dimensional lattice. Among clusters larger than Cd-54, MOL-5 is the closest to Cd-54 in terms of the unit cell size, and it crystallizes into a primitive cubic cell (29.90 Å). As shown in Figure 3, compared to that in the Cd-54 cluster, its diffraction peaks shift toward the low angle due to the larger unit cell, and the optical absorption peaks shift toward the longer wavelength due to the quantum size effect. These data suggest that MOL-5 is a homologous member after the Cd-54 cluster in the C*n* (or C*n*,*m*) series. The two successive members after Cd-54 are Cd-84 and Cd-123 with ideal compositions of $[Cd_{84}S_{59}(SPh)_{60}L_4]^{10-}$ and $[Cd_{123}S_{96}(SPh)_{72}L_4]^{18-}$ (L = neutral ligand), respectively. On

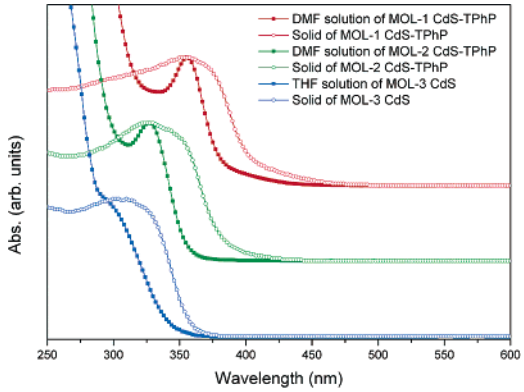

Figure 4. Quantum confinement effects shown by UV−vis spectra for solution and solid samples containing tetrahedral clusters of different sizes.

the basis of the trend in the cubic unit cell length (29.90 Å for MOL-5, 24.0656(7) Å for the Cd-54 cluster, and 21.856(2) Å for the Cd-32 cluster), it appears that MOL-5 is more likely to be related to Cd-123 than Cd-84.

The availability of this family of quantum dots and their superlattices makes it possible to probe effects of subtle compositional and structural variations on their optical properties. Of particular interest is the size-dependent quantum confinement effect demonstrated in Figures 3 and 4.[20] For example, in Figure 4, the solution of MOL-1 CdS−TPhP (Cd-54) shows an absorption peak with the maximum at 353 nm. In comparison, the absorption peak for the solution containing Cd-32 clusters from MOL-2 is blue-shifted to 327 nm, as expected from the quantum size effect. The solution with Cd-17 clusters shows a less-well-defined peak around 291 nm that may contain contributions from absorption by surface ligands.

Crystalline solids and their solutions exhibit significantly different spectra, attributable to the intercluster interaction (Figure 4). For example, for MOL-1 CdS−TPhP with Cd-54 clusters, the absorption peak of the solid sample is broader, and the onset of the absorption is red-shifted to the longer wavelength, compared to the spectrum of its DMF solution. The similar difference between solid and solution samples is also found for Cd-32 or Cd-17 clusters (Figure 4).

In conclusion, a general synthetic method has been developed and demonstrated to be effective in the synthesis of cadmium sulfide quantum dots of various sizes, compositions, and structures. Compared to other synthetic approaches for nanocrystal synthesis, this method is advantageous in its ability to prepare single-sized quantum dots with high crystallinity, making it feasible to probe detailed atomic structures with single-crystal diffraction. With the generalized synthetic method reported here, we anticipate further synthetic breakthroughs in the synthesis of even larger quantum dots with a precise number of atoms and their superlattices and in the applications of these single-sized quantum dots.

Acknowledgment. We thank the support of this work by NSF (P. F.) and the donors of the Petroleum Research Fund (administered by the ACS) (X.B. and P.F.). P.Y. is an Alfred P. Sloan research fellow, Beckman Young Investigator, and Camille Dreyfus Teacher-Scholar.

Supporting Information Available: Crystallographic data, including positional parameters, thermal parameters, and bond distances and angles (CIF). This material is available free of charge via the Internet at http://pubs.acs.org.

References

(1) Dance, I. G.; Fisher, K. *Prog. Inorg. Chem.* **1994**, *41*, 637−803.
(2) Soloviev, V. N.; Eichhofer, A.; Fenske, D.; Banin, U. *J. Am. Chem. Soc.* **2001**, *123*, 2354−2364.
(3) Krebs, B., Henkel, G. *Angew. Chem., Int. Ed.* **1991**, *30*, 769−788.
(4) Doellefeld, H.; Weller, H.; Eychmueller, A. *J. Phys. Chem. B* **2002**, *106*, 5604−5608.
(5) Murray, C. B.; Kagan, C. R.; Bawendi, M. G. *Science* **1995**, *270*, 1335−1338.
(6) Scott, R. W. J.; MacLachlan, M. J.; Ozin, G. A. *Curr. Opin. Solid State Mater. Sci.* **1999**, *4*, 113−121.
(7) Dhingra, S.; Kanatzidis, M. G. *Science* **1992**, *258*, 1769−1772.
(8) Cahill, C. L.; Parise, J. B. *J. Chem. Soc., Dalton Trans.* **2000**, 1475−1482.
(9) Li, H.; Laine, A.; O'Keeffe, M.; Yaghi, O. M. *Science* **1999**, *283*, 1145−1147.
(10) Zheng, N.; Bu, X.; Feng, P. *Nature* **2003**, *426*, 428−432.
(11) Zheng, N.; Bu, X.; Wang, B.; Feng, P. *Science* **2002**, *298*, 2366−2369.
(12) Dameron, C. T.; Reese, R. N.; Mehra, R. K.; Kortan, A. R.; Carroll, P. J.; Steigerwald, M. L.; Brus, L. E.; Winge, D. R. *Nature* **1989**, *338*, 596−597.
(13) Lee, G. S. H.; Craig, D. C.; Ma, I.; Scudder, M. L.; Bailey, T. D.; Dance, I. G. *J. Am. Chem. Soc.* **1988**, *110*, 4863−4864.
(14) Vossmeyer, T.; Reck, G.; Katsikas, L.; Haupt, E. T. K.; Schulz, B.; Weller, H. *Science* **1995**, *267*, 1476−1479.
(15) Herron, N.; Calabrese, J. C.; Farneth, W. E.; Wang, Y. *Science* **1993**, *259*, 1426−1428.
(16) Vossmeyer, T.; Reck, G.; Schulz, B.; Katsikas, L.; Weller, H. *J. Am. Chem. Soc.* **1995**, *117*, 12881−12882.
(17) Behrens, S.; Bettenhausen, M.; Deveson, A. C.; Eichhoefer, A.; Fenske, D.; Lohde, A.; Woggon, U. *Angew. Chem., Int. Ed. Engl.* **1996**, *35*, 2215−2218.
(18) A typical synthesis condition is given below using MOL-1 CdS−TPhP as an example; 42 mg of PPh_4Br, 49 mg of thiourea, 189 mg of $Cd_4(SPh)_8$, 424 mg of water, and 2.570 g of CH_3CN were mixed in a 23 mL Teflon-lined stainless steel autoclave and stirred for ~20 min. The vessel was then sealed and heated at 150 °C for 3 days. After cooling to room temperature, 122 mg of MOL-1 CdS−TPhP crystals was obtained as large cubic crystals.
(19) Feng, P.; Bu, X.; Zheng, N. *Acc. Chem. Res.* **2005**, *38*, 293−303.
(20) Alivisatos, A. P. *J. Phys. Chem.* **1996**, *100*, 13226−13239.

JA053588O